A Study on the Dynamic Analysis and Control Algorithm for a Motor Driven Power Steering System

Seokchan Yun, Changsoo Han*
Department of Precision Mechanical Engineering, Hanyang University, Sa 1 dong, 1271 Ansan, Kyonggi-do, 425-791, Korea
Durkhyun Wuh
KATECH, Yongjeong 74, Poongse-myeon, Cheonan, Chungnam 330-912, Korea

The power steering system for vehicles is becoming essential for supporting the steering efforts of the drivers, especially for the parking lot maneuver. Although hydraulic power steering has been widely used for years, its efficiency is not high enough. The problems associated with a hydraulic power steering system can be solved by a motor driven power steering (MDPS) system. In this study, a dynamic model and a control algorithm for the ball screw type of MDPS system have been derived and analyzed by using the method of discrete modeling technology. To improve steering feel and power steering characteristics, two derivative gains are added to the conventional power boosting control algorithm. Through simulations, the effects of the control gain on the steering angle gain were verified in the frequency domain. The steering returnability and steering torque phase lag in on-center handling test were also evaluated in the time domain.

Key Words : Motor Driven Power Steering (MDPS), Ball Screw, Control Algorithm, Steering Angle Gain, Returnability, Phase Lag

Nomenclature

K_{tb}, K_{sl} : (Nm/rad) : Torsion bar and steering linkage stiffness
B_{sw}, B_{fw} : (Nm/(rad/sec)) : Viscous damping coefficient of steering wheel and front wheel
B_m : (Nm/(rad/sec)) : Viscous damping coefficient of motor
J_{sw}, J_{fw} : ($kg \cdot m^2$) : Moment of inertia of steering wheel and front wheel
J_m, J_p : ($kg \cdot m^2$) : Moment of inertia of motor armature, pinion
M_{sl} : (kg) : Mass of steering linkage
r_1 : (m) : Rack and Pinion ratio (Pinion Radius)
r_2 : (1/m) : Steering Linkage ratio
r_3 : (m/rad) : Ball Screw ratio (lead/rad)
K_m : (Nm/A) : Motor constant
G : (V/deg.) : Torque Sensor Gain
η : (Dimensionless) : Torque transmission efficiency of gearbox
T_{sw} : (N. m) : Steering input torque
AT : (N. m) : Aligning torque
I_{in} : (A) : Motor input current
θ_{sw}, θ_{fw} : (rad) : Steering wheel and front wheel angle
X_{sl} : (m) : Displacement of steering linkage(rack bar)

* Corresponding Author.
E-mail : cshan@hanyang.ac.kr
TEL : +82-31-400-5247; **FAX** : +82-31-406-6242
Department of Mechanical Engineering, Hanyang University, Sa 1 dong, 1271 Ansan, Kyunggi-do 425-791, Korea. (Manuscript **Received** January 22, 2001; **Revised** November 15, 2001)

1. Introduction

The ease of driving is a major design consideration for automobiles. Therefore, there are more and more automobiles equipped with hydraulic power steering every year. This trend is mainly due to the current requirement of the ease of driving. In particular, using power assisted technologies for various controls (e.g. speed-sen-

sitive power assist) is a current trend which has a strong influence on car design (Nakayama, 1994). The power steering system assisting the steering effort of the vehicle is aimed at relieving the driver's steering effort when the vehicle is either at rest or in low velocity. When the contact friction of the tire is reduced with high velocity driving, the steering effort is weak and the steering stability becomes worse. To prevent this, either the assisted steering effort should be reduced or the steering wheel should be held tight (Shimizu, 1991; Nakayama, 1994). To meet this requirement, an electrically controlled hydraulic power steering (ECPS) system was developed. The ECPS system, however, is more expensive and heavier than the conventional hydraulic power steering system. For this reason, a motor driven power steering (MDPS) system with a steering column which assists the steering effort according to vehicle velocity was designed and tested. Motor power density and motor control problems, however, were the obstacles in developing the MDPS system. These days, there has been considerable progress in the field of power electrronics where the trend is moving towards small components with increased power density, and in the field of microelectronics where microcontrollers with high computing performance are used (Schleuter, 1989). The inertia of the motor armature and the friction of the steering system influence the steering performance, the steering feel, and the performance of the moving vehicle. Due to the limitations of the motor capacity, it has only been applied to light vehicles. To be applied to a mid-size vehicle, the ball-screw-typed MDPS system, which directly joins the rack bar, was proposed. This was done by mounting on the rack bar (Shimizu, 1991; Nakayama, 1994). In this paper, a model of the ball-screw -typed MDPS system was derived and a controller was designed. The steering angle gain was defined as the performance index, which indicated the steering characteristics. The effectiveness of the controller was examined by investigating the influence on the performance indices of the controller in the frequency and time domains.

2. System Description

The steering system is a complex one that consists of spring elements such as the torsion bar, the damping element of each joint, and the nonlinear spring-damping element such as the bushing. Our goal is deriving the MDPS system model with proper degrees of freedom to analyze the steering system, to evaluate the steering stability of the vehicle, and to design a control algorithm for the MDPS system.

2.1 System modeling

The MDPS system detects the steering torque from the torque sensor by generating the voltage signal according to the steering input as the driver turns steering wheel. It also senses the velocity of the vehicle from the pulse signal generated by the velocity sensor. It also controls the electric current of the motor in order to produce the proper assisting power. The control mechanism produces an electric current in response to the velocity of the vehicle. It maintains normal operation of the steering system even the system is malfunctioning. Basically, this system consists of torque sensors, velocity sensors, a control device, motors, reduc-

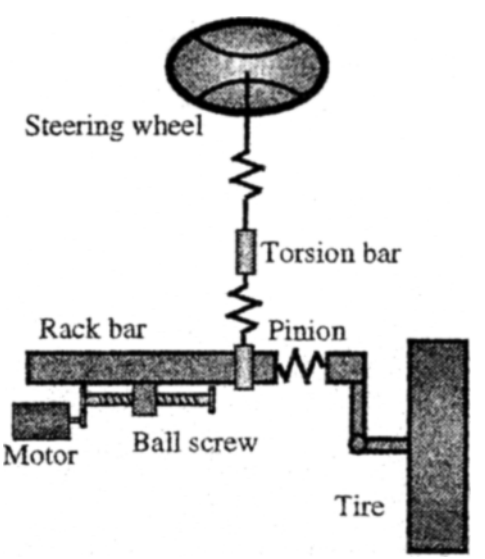

Fig. 1 Schematic of a ball screw type of MDPS system

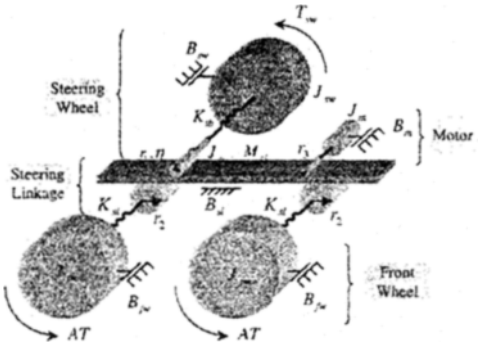

Fig. 2 The lumped mass model for a ball screw type of MDPS

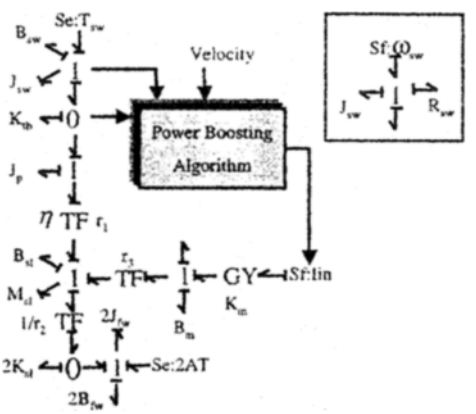

Fig. 3 The bond graph model for a ball screw type of MDPS system

tion gears, and ball screws. Figure 1 shows the schematic of the system.

For the modeling of the steering system, inertia elements (steering wheel, steering linkages, front wheel and motor armature), damping coefficient of each part and stiffness (steering column and links) are considered. The lumped mass model of the steering system is shown in Fig. 2.

The modeling process of the system will be explained by using of the bond graph method (Karnopp, 1990). The bond graph is a useful analysis tool for a system which behaves in a complex physical domain, such as the MDPS system. The bond graph model for the MDPS system is illustrated in Fig. 3.

As shown in Fig. 3, the pinion and the rotor of the motor move dependently in a rack bar, so they have derivative causality. The total 3-degrees-of-freedom dynamic equations are obtained from the bond graph model.

$$J_{sw}\ddot{\theta}_{sw}+B_{sw}\dot{\theta}_{sw}+K_{tb}\left(\theta_{sw}-\frac{1}{r_1}X_{sl}\right)=T_{sw} \quad (1)$$

$$M_{SL}\ddot{X}_{sl}+B_{SL}\dot{X}_{sl}+K_{SL}X_{sl}-\eta\frac{K_{tb}}{r_1}\theta_{sw}-2\frac{K_{sl}}{r_2}\theta_{fw}=\frac{1}{r_3}K_mI_m \quad (2)$$

$$J_{fw}\ddot{\theta}_{fw}+B_{fw}\dot{\theta}_{fw}+K_{sl}\theta_{fw}-\frac{K_{sl}}{r_2}X_{sl}=AT \quad (3)$$

where, M_{SL}, B_{SL}, and K_{SL} represent, respectively, the equivalent inertia, damping, and the stiffness required to convert the rotating motion of the pinion and the motor into the linear motion of the rack bar. They are shown in the following equations.

$$M_{SL}=M_{sl}+\eta\frac{J_p}{r_1^2}+\frac{J_m}{r_3^2} \quad (4)$$

$$B_{SL}=B_{sl}+\frac{B_m}{r_3^2} \quad (5)$$

$$K_{SL}=2\frac{K_{sl}}{r_2^2}+\eta\frac{K_{tb}}{r_1^2} \quad (6)$$

where r_3 represents the moving distance of the rack bar with unit of rotational angle of the ball screw, which is less than 1. As in Eq. (4), the influence of the motor inertia becomes increased, because the motor inertia is inversely proportional to the square of r_3. This problem can be solved somewhat by increasing the pitch of the ball screw mechanically. Its size, however, should be limited because it is inversely proportional to the output capacity of the motor.

If the steering input is the steering angle instead of the driver's torque, the steering wheel must have the derivative causality. The steering angle (θ_{sw}) and the electric current of the motor(I_m) become the inputs.

2.2 Verifications of model

For the verification of the model, a computer simulation was carried out by combining the steering system model with the whole vehicle model. For deriving the control algorithm, it is important to derive a vehicle model with a proper degrees of freedom. A model with too many degrees of freedom may negatively influence the evaluation. To investigate the stability of the vehicle, a whole vehicle model, which can dem-

Table 1 D.O.F. of full vehicle model

		Parameter	No.of Part	D.O.F.
Body		x, y, yaw, roll	1	4
Wheel	Spin	φ	4	4
	Steer	ϕ		1
Total		9D.O.F.		

Table 2 Full vehicle model parameters

Parameter	Value	Unit
Vehicle(sprung) mass	1245(1045)	kg
Yaw moment of intertia of vehicle	2014	kgm^2
Dist. from C.G. to front, rear axle	1.290, 1.37	m
Front, rear track width	1.42, 1.42	m
Front, rear cornering stiffness	38400, 30666	N/rad
Tire rolling resistance coeff.	0.012	Dim.less
Front, rear roll stiffness	37356,31420	Nm/rad.
Front, rear roll damping	1600, 1600	Nms/rad.
Distance from C.G.to roll axis	0.4	m

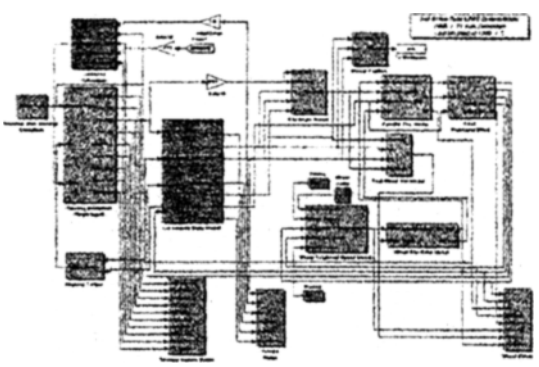

Fig. 4 Simulink model of the entire system

onstrate detailed motion according to the steering will be needed. The degrees of freedom used for the vehicle model is indicated in Table 1. Vehicle parameters used in the simulation are shown in Table 2. For the simulation, the vehicle model with the proposed steering model is represented by the Simulink™ as in Fig. 4.

The verification of the MDPS system was done by comparing those values of the yaw rate and lateral acceleration, which are the important states of the vehicle. The J-turn test is one of the ISO evaluation methods used to check the vehicle' s status in a sudden steering change (ISO 7401,

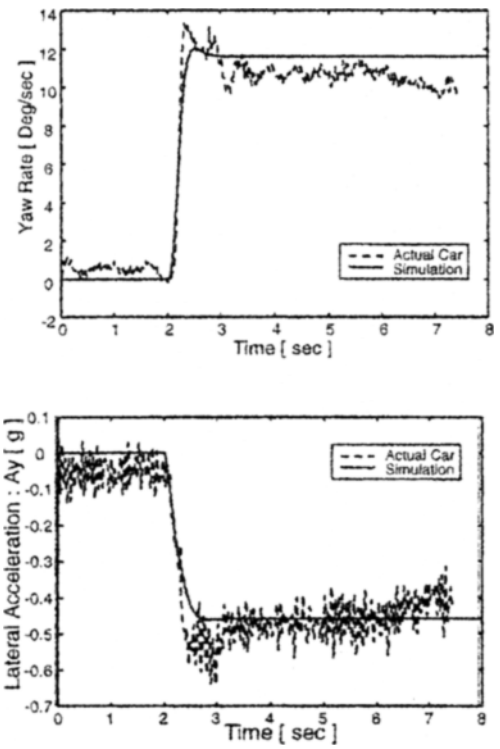

Fig. 5 J-turn test

1988). In this study, the vehicle will be driven at 80km/h for two seconds and then a steering input of 45°within 0.2 seconds will be applied. The yaw rate and the lateral acceleration of the vehicle are measured from the C. G. of the vehicle body by using sensors.

Figure 5 shows the simulated comparisons of the yaw rate and the lateral acceleration with the measured data of the vehicle. The simulation values are almost the same as the test results with respect to magnitudes and overall shapes. From the results, it appears that the computer model of steering simulation is quite reasonable (Yun, 2000).

3. Control and Simulation

3.1 Control algorithm

The basic driving algorithm is the velocity boosting control, which operates according to the vehicle velocity and the steering torque. To obtain the control gain, the steering effort for a giver

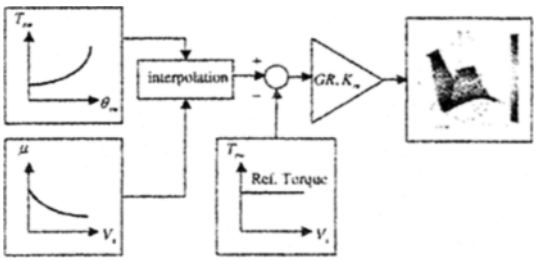

Fig. 6 Calculation algorithm for speed-sensitive gain curve

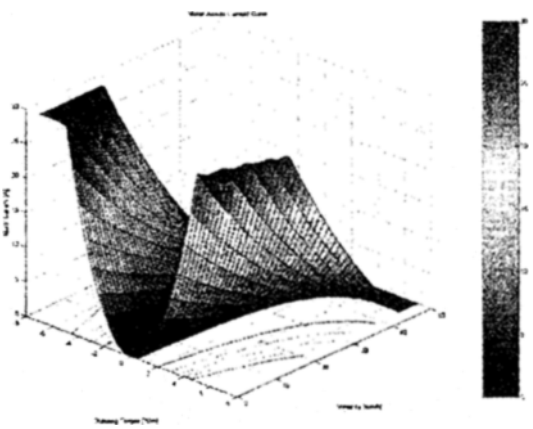

Fig. 7 Basic speed-sensitive gain curve

vehicle velocity and the steering angle are necessary. The required steering effort can be obtained by subtracting the steering torque that a driver can handle (Yun, 2000). The electric current for the velocity, the steering torque and the gear ratio are needed to be calculated. Fig. 6 shows the calculation algorithm for a speed sensitive gain curve and Fig. 7 represents the control gain map based on these processes. It is a basic torque boosting gain (K_p) of the steering torque and vehicle speed input. This gain is proportional to the steering torque and inversely proportional to the vehicle speed.

As mentioned, reducing the steering effort is possible by applying the gain, but new control items may be needed to make the steering feel better. The steering torque rate (K_{d1}) gain is introduced to improve the driver's feedback torque and the effect of the inertia of the motor. The steering angular rate (K_{d2}) gain is introduced for controlling the damping effect, the

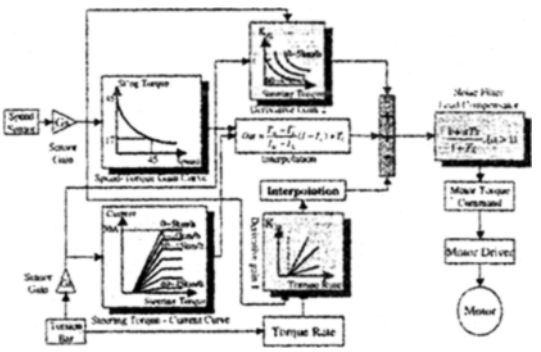

Fig. 8 Control block diagram

returnability, and the basic velocity induction controller. The tire friction is a function of vehicle velocity. It is closely related to the performance indices such as returnability and phase lag. So, the derivative gain is also a function of vehicle velocity. The following equation shows the combined control items:

$$I_{in}=K_pG\left(\theta_{sw}-\frac{r_2}{r_1}\theta_{fw}\right)+K_{d1}G\left(\dot{\theta}_{sw}-\frac{r_2}{r_1}\dot{\theta}_{fw}\right)+K_{d2}\dot{\theta}_{sw} \quad (7)$$

Using the above driving algorithm, Fig. 8 shows the block diagram to actuate the real motor (Yun, 2000). In order to embody Eq. (7) in ECU, many factors must be pre-calculated for the practical reason. By considering costs and efficiency, control gains are stored as a look-up table in memory and interpolated. In Fig. 8, 'Speed-Torque gain curve' block and 'Steering torque-current curve' block are interpolated and used for the calculation of speed sensitive boosting gain K_p. 'Derivative gain 1' block represents steering torque rate gain (K_{d1}) and 'Derivative gain 2' block does steering wheel rate gain (K_{d2}). This algorithm determines the assist power by interpolating both the graph of the steering torque versus the velocity and the graph for the steering torque versus the electric current of the motor. In this algorithm, the power boosting gain acts in the direction of decreasing torque. The steering torque rate gain is working to the opposite direction of steering torque rate. The steering wheel rate gain is working to the opposite direction of steering angular velocity. K_{d1} and K_{d2} can be calculated from the steering angle gain response according to the steering

frequency. Note that K_{d1} must be decreased and K_{d2} must be increased as the steering frequency is increased (Yun, 2000). In this study K_{d1} and K_{d2} are tuned based on the vehicle speed.

3.2 Steering angle gain

The motor driven power steering system has several characteristics and merits. One weak point in the design is that the steering feel is not good when compared with the conventional hydraulic power steering. The steering feel is related with driver's feedback torque. An equation, which relates the steering motion and the reaction torque, is needed in order to illustrate steering feel. In this paper, as in Eq. (8), the steering angle gain that indicates the steering angle(θ_{sw}) and the reaction torque(T_{sw}) by the form of the transfer function will be used as the index of the steering feel (Chikuma, 1992). The steering angle and the reaction torque can be derived from the bond graph in Fig. 3 and these values are used in the following equation.

$$G_h=\frac{T_{sw}}{\theta_{sw}} \tag{8}$$

Detailed derivation of the steering angle gain is summarized in the Appendix. This index is always a kind of acausal transfer function. Hence, the analysis of this index is somewhat different from that of the causal transfer function. The magnitude of the steering angle gain represents the magnitude of the driver's feedback torque for the steering angle input. Good steering system needs uniform feedback torque response in a steering feel aspect. It requires uniformly distributed shape of magnitude of steering angle gain in overall frequency region.

3.3 Frequency domain response

To evaluate the performance of the proposed algorithm with the general power assisting control algorithm, the frequency response analysis of Eq. (8), which indicates the steering characteristics, will be performed.

3.3.1 The effect of motor armature inertia

Generally, one of the elements that affects the steering feel is the inertia of the rotor in motor. Fig. 9 shows the steering angle gain due to an armature inertia. As shown in this figure, the effect of the motor inertia is small due to the low gear ratio and the slow rotating velocity in the ball screw type MDPS system.

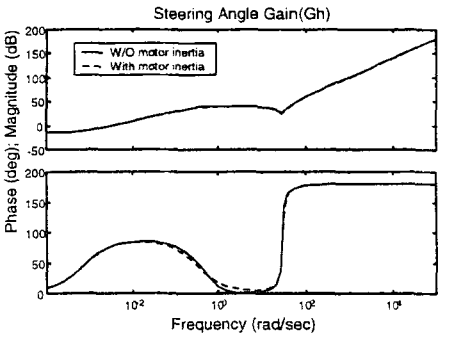

Fig. 9 The effect of motor armature inertia

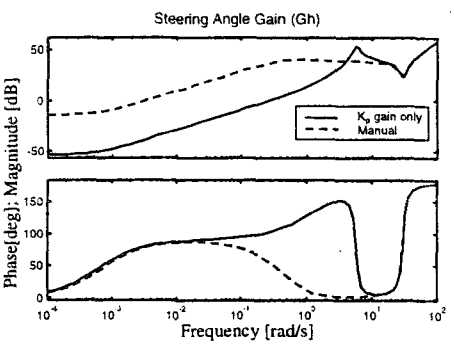

Fig. 10 Power boosting characteristics

3.3.2 Power boosting characteristics

The frequency response due to the power assist is shown in Fig. 10. By comparing the magnitudes of steering angle gain, we can say that the driving power is assisted because the magnitude is lowered. The magnitude response in the high frequency region, however, shows uneven shape and indicates that more steering effort needed compared with the manual steering. So, power boosting gain(K_p) makes system characteristics worse in the high frequency region.

3.3.3 Effect of differential gain 1(K_{d1})

Figure 11 demonstrates the effect of differential gain 1 in the control algorithm Eq. (7). In this

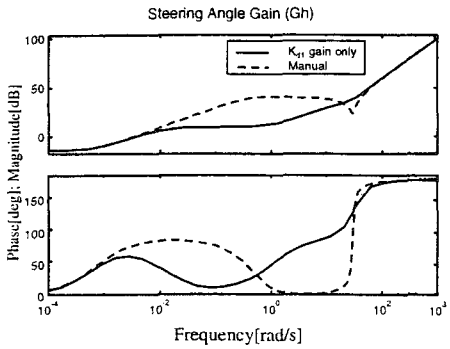

Fig. 11 Effect of K_{d1} gain

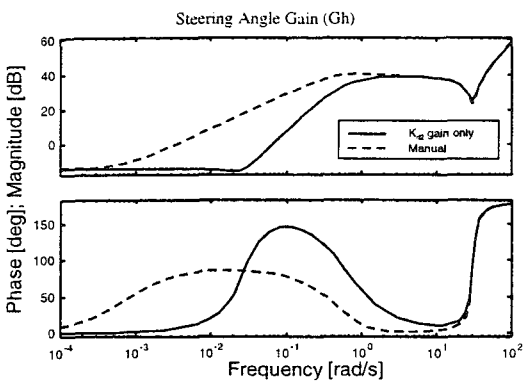

Fig. 12 Effect of K_{d2} gain

test, the controller which has only K_{d1} gain is compared with the manual steering. As shown in this figure, this gain improves the response in the high frequency region, which was worsened by the previously adjusted power assist gain.

3.3.4 Effect of differential gain 2(K_{d2})

Figure 12 shows the effect of differential gain 2. In this test, the controller with only K_{d2} gain is compared with the manual steering. This gain plays an important role by keeping the magnitude of steering angle gain uniformly in the low frequency region. By applying this gain, the uniform steering angle response can be obtained in the low frequency band.

3.3.5 Effect of all the control gain

Figure 13 illustrates the results with all the control gains are applied. The responses in overall frequency regions become constant. From the above results, it is shown that the proposed control algorithm works quite effectively.

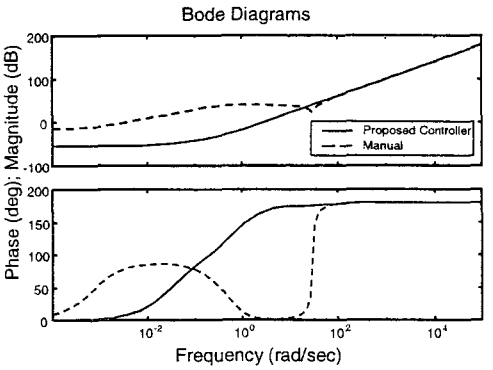

Fig. 13 Control effect of all control gain

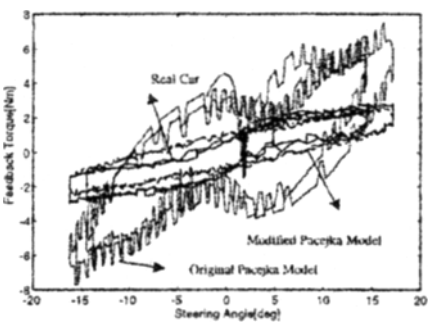

Fig. 14 Compensated tire model

3.4 Time domain response

In order to investigate several steering characteristic responses(such as the steering effort, returnability, and time lag as well as the response of vehicle to the steering angle input), an almost exact model of the steering system of the actual vehicle will be needed. The steering system of the actual vehicle has too many complicated elements to model precisely; like as the bushing, the non-linear friction, and the steering effect of the suspension system. Most of the analytical tire models generate accurate forces and moments in the viewpoint of the vehicle motion amalysis. However, these forces and moments show some inaccuracy in the aspect of steering system analysis. Most of the conventional tire models show differences in magnitude and phase of the steering feedback torque compared with actual car. In this study, we compensated for the steering effort in the simulation model to obtain a reliable

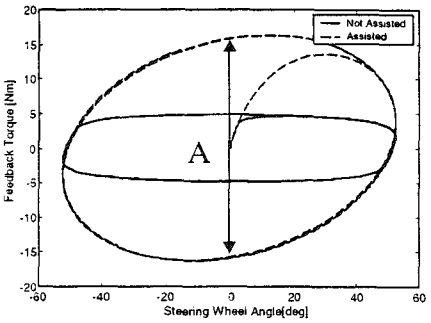

Fig. 15 On-center handling test

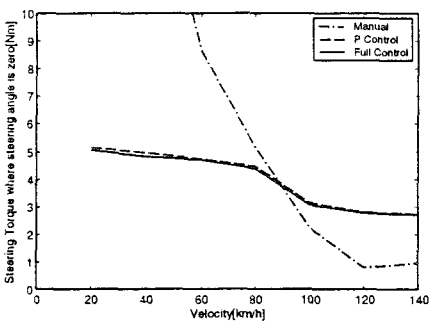

Fig. 16 Quantitative evaluation of steering torque

response by measuring and applying the force value that acts in the rack bar based on the velocity and the steering angle of the actual car. Figure 14 shows the driver's feedback torque comparison between the actual car and simulation models in a slalom test at V=100km/h. From this figure, we can say that the modified Pacejka tire model can produce almost exact feedback torque compared with the test result. Hence, modified Pacejka tire model enables us to derive reasonable results.

The sinusoidal steering input with the maximum lateral acceleration of approximately 0.2g and the steering frequency of 0.2Hz is put to a test. Figure 15 shows the graph of the steering angle versus the steering torque. In this graph, the value of the steering torque (A part in Fig. 15), when the steering angle is zero, shows the steering effort at the steering wheel when a driver turns it (Norman, 1984; Sato, 1991). Figure 16 shows the quantitative evaluation of the steering feedback torque for the maximum lateral acceleration of approximately 0.2g. Note that the manual steering

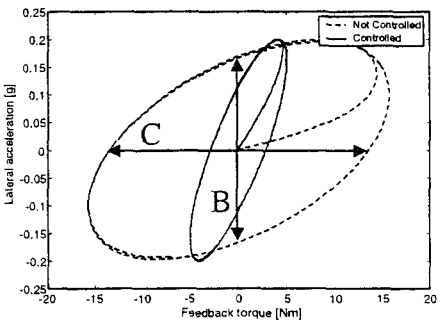

Fig. 17 Steering torque vs. Lateral acceleration plot

makes the steering effort too high at low velocity and too low at high velocity. The relatively uniform steering effort is obtained in the full speed range when the controller is operated. The proposed controller in this study, however, compared with the general P controller, decreases the steering effort slightly when the control gain of the derivative terms is added.

Figure 17 shows the steering torque versus the lateral acceleration graph when the sinusoidal steering input is added. The dotted line indicates the simple power boosting control and the continuous line indicates the control input proposed in this study. In this figure, the lateral acceleration (when the steering torque is 0 (B part)) is the index that measures the returnability of the steering system (Norman, 1984; Sato, 1991). Figure 18 shows the quantitative evaluation of the steering returnability at different velocities. In the case where the characteristic value (B part) is too small, the steering returnability becomes excessive and the driver tends to feel that the reaction force of the steering wheel is too high. If the characteristic value (B part) is too high, on the contrary, the driver tends to feel that the reaction force of the steering wheel is insufficient (Norman, 1984; Sato, 1991). For the verification of the proposed control algorithm, the steering angle is turned for a maximum lateral acceleration of approximately 0.2g. In case of manual steering, the returnability becomes worse at low velocity and it becomes excessive at high velocity. Although the returnability at high velocity is still excessive, the performance of the proposed con-

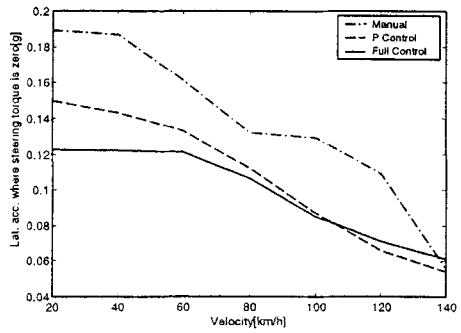

Fig. 18 Quantitative evaluation of steering returnability

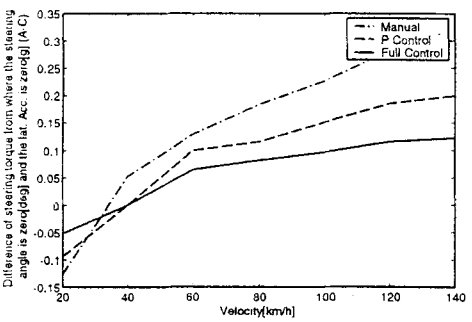

Fig. 19 Quantitative evaluation of steering torque phase lag

troller becomes better compared with the case of the manual steering. The proposed controller, however, improve the returnability at the low velocity and restrains the returnability at the high velocity. Thus it can maintain the uniform returnability regardless of the velocity.

The value that subtracts the steering effort, when the lateral acceleration is zero, from the steering effort of a driver(A-C) is the index that indicates the phase lag of the driver's torque (Sato, 1991). Figure 19 shows the quantitative evaluation of the steering torque phase lag at different velocities. From the test results, we may conclude that the controller proposed in this paper shows very good phase lag performance.

4. Conclusion

A dynamic model and an assisting motor algorithm for the ball screw type MDPS system have been derived and analyzed. A summary of the results is as follows:

(1) By using the bond-graph, a dynamic model for the ball-screw type MDPS system is developed. This steering system has a total of 3 D. O. F. and has been joined with a full car model. The proposed model is verified with the J-turn test results of an actual car.

(2) In order to enhance the control performance, an assisting motor controller is designed for the system. The proposed controller consists of the power boosting gain (K_p) which is proportional to the steering torque , derivative gains which are proportional to the steering torque rate (K_{d1}) and the steering angular rate (K_{d2}). The power boosting gain was calculated from the tire and steering dynamics. The steering torque gain and the steering angular rate gain are functions of vehicle speed and tuned at each vehicle speed.

(3) The steering angle gain that is the performance index of the steering characteristics is defined. Through computer simulation, the characteristics of frequency response for the steering angle gain of each control element for the proposed controller is analyzed. The K_p gain represents the power assisting property, however, this gain makes the system dynamics worse at the high steering frequency region of 4~8(rad/s). The K_{d1} gain improves the response in the high frequency region, which is worsened by the K_p gain. The K_d gain makes the magnitude of steering angle gain uniform in the low frequency region. By applying this gain, the uniform steering angle response can be obtained in the low frequency band.

(4) The conventional simple torque boosting controller shows bad characteristics in returnability and phase lag in overall speed range. The proposed controller designed in the time-domain maintains the comparatively uniform returnability regardless of the vehicle speed. This controller also shows the enhanced steering returnability and the reduced steering torque phase lag at various vehicle speed.

References

Baxter, J., 1989, "Analysis of Stiffness and Feel

for a Power-Assisted Rack and Pinion Steering Gear," *SAE880706*, pp. 827~833.

Chikuma, I. and Shimada, S., 1992, "Electric Power Steering for Passenger Car," *NSK Technical Journal* No. 654, pp. 36~47.

Dixson, J. C., 1991, *Tires, Suspension and Handling*, Cambridge University Press.

ISO 7401, 1988, *1988 Road Vehicles-Transient Open-Loop Response Test with Step Steering.*

Jang, J. H. and Han, C. S., 1997, "The Sensitivity Analysis of Yaw Rate for the Front Wheel Steering Vehicle: In the Frequency Domain," *KSME International Journal*, Vol. 11, No. 1, KSME, pp. 56~66.

Jang, J. H and Han, C. S., 1997, "Sensitivity Analysis of Side Slip Angle for a Front Wheel Steering Vehicle: a Frequency Domain Approach," *KSME International Journal*, Vol. 11, No. 4, KSME, pp. 367~378.

Karnopp, D. C., Margolis, D. L. and Rosenberg, R. C., 1990, *System Dynamics: A Unified Approach, 2 nd Ed.*, John Wiley & Sons Inc.

Lee, S. H., Lee, U. K., Han, C. S., 1999, "Four-wheel Independent Steering(4WIS) System for Vehicle Handling Improvement by Active Rear Toe Control," *JSME International Journal*, Vol. 42, No. 4.

Nakayama, T. and Suda, E., 1994, "The Presence and Future of Electric Power Steering," *International Journal of Vehicle Design*, Vol. 15, Nos 3/4/5, pp. 243~254.

Norman, K. D., 1984, "Object Evaluation of On-Center Handling Performance," *SAE840069*, pp. 1~13.

Sato, H., et al., 1991, "The Quantitative Analysis of Steering Feel," *JSAE review* Vol. 12, No. 2, pp. 85~87.

Schleuter, W., 1989, "Electric Servo Drive for Front and Rear Wheel Power Steering," *Journal of Automobile Engineering*, C382/065, ImechE, pp. 361~368.

Shimizu, Y. and Kawai, T., 1991, "Development of Electric Power Steering," *SAE910014*, pp. 105~119.

Takehara, S., et. Al., 1997, "Improvement of Motor Inertia Influence of Electric Power Steering," *Proceedings of Automotive Technology*, pp. 69~72 (in Japanese).

Yun, S. C, 2000, "A Study on the Enhanced Control Algorithm for a Ball Screw Type of Motor Driven Power Steering System," Ph. D. Thesis, Hanyang University.

Appendix

The steering angle gain of the MDPS system of Eq. (8) is derived as follows. Steering angle gain is the function of the steering system parameters and the aligning torque.

$$G_h = \frac{A_1S^6+A_2S^5+A_3S^4+A_4S^3+A_5S^2+A_6S^1+A_7}{B_1S^4+B_2S^3+B_3S^2+B_4S^1+B_5}$$

where,

$$A_1 = -J_{fw}J_{sw}M_{SL}r_1^2r_2^2r_3$$

$$A_2 = (B_{sw}/J_{sw}+B_{fw}/J_{fw}+B_{SL}/M_{SL})A_1$$

$$A_3 = \left\{\frac{1}{M_{SL}}\left(K_{SL}+\frac{B_{SL}B_{sw}}{J_{sw}}+\frac{B_{fw}B_{SL}}{J_{fw}}+\frac{GK_mK_p}{r_1r_3}\right)+\frac{B_{fw}B_{sw}+J_{fw}K_{tb}+J_{sw}K_{sl}-J_{sw}K_{at}}{J_{sw}J_{fw}}\right)A_1$$

$$A_4 = A_1(B_{sw}GK_mK_p-K_{d2}K_{tb}/r_1+B_{fw}B_{SL}B_{sw}/J_{fw}+B_{sw}K_{SL}+B_{SL}K_{tb})/M_{SL}J_{sw}+A_1(B_{fw}GK_mK_p/r_1r_3-B_{SL}K_{at}+B_{SL}K_{sl}+B_{fw}K_{SL})/M_{SL}J_{fw}+A_1(B_{sw}K_{sl}-B_{sw}K_{at}+B_{fw}K_{tb})/J_{sw}J_{fw}$$

$$A_5 = GK_mK_pr_1r_2^2(J_{sw}K_{at}-B_{fw}B_{sw}-J_{sw}K_{sl})+(K_{at}-K_{sl})B_{SL}B_{sw}r_1^2r_2^2r_3+(\eta J_{fw}K_{tb}/r_1^2+B_{fw}K_{d2}/r_1-B_{fw}B_{SL}-J_{fw}K_{SL}+K_{at}M_{SL}-K_{sl}M_{SL})K_{tb}r_1^2r_2^2r_3+\{2J_{sw}K_{sl}K_{SL}/r_2^2+(J_{sw}K_{at}-B_{fw}B_{sw}-J_{sw}K_{sl})K_{SL}\}r_1^2r_2^2r_3$$

$$A_6 = \{(K_{at}-K_{sl})B_{sw}GK_mK_p/r_1r_3+(2K_{sl}/r_2^2+K_{at}-K_{sl})B_{sw}K_{SL}\}r_1^2r_2^2r_3+(\eta B_{fw}/r_1^2-K_{at}K_{d2}/r_1+K_{d2}K_{sl}/r_1+B_{SL}K_{at}-B_{SL}K_{sl}-B_{fw}K_p)K_{tb}r_1^2r_2^2r_3$$

$$A_7 = \eta(K_{sl}-K_{at})K_{tb}^2r_2^2r_3+(2K_{sl}/r_2^2+K_{at}-K_{sl})r_1^2r_2^2r_3$$

$$B_1 = J_{sw}M_{SL}r_1^2r_2^2r_3$$

$$B_2 = (B_{SL}/M_{SL}+B_{fw}/J_{fw})B_1$$

$$B_3 = (GK_mK_p/M_{SL}r_1r_3+B_{fw}B_{SL}/M_{SL}J_{fw}+K_{SL}/M_{SL}-K_{at}/J_{fw}+K_{sl}/J_{fw})B_1$$

$$B_4 = (B_{fw}GK_mK_p/r_1r_3-B_{SL}K_{at}+B_{SL}K_{sl}+B_{fw}K_{SL})r_1^2r_2^2r_3$$

$$B_5 = (K_{sl}-K_{at})GK_mK_pr_1r_2^2+(K_{sl}-K_{at}-2K_{sl}/r_2^2)r_1^2r_2^2r_3$$